Universidade de Brasília

Computational fluid dynamics simulations guided by 3D PC-MRI data

Vinicius C. Rispoli[1] (vrispoli@pgea.unb.br), Jon F. Nielsen[2] (jfnielse@umich.edu)
Krishna S. Nayak[3] (knayak@usc.edu), Joao Luiz A. Carvalho[1] (joaoluiz@pgea.unb.br)

[1]Department of Electrical Engineering, University of Brasilia, Brasilia, DF, Brazil
[2]Biomedical Engineering, University of Michigan, Ann Arbor, MI, USA
[3]Electrical Engineering, University of Southern California, Los Angeles, CA, USA

PGEA PÓS-GRADUAÇÃO EM ENGENHARIA DE SISTEMAS ELETRÔNICOS E DE AUTOMAÇÃO

GPSIM Grupo de Processamento de Sinais e Imagens Médicas

Introduction

- Phase contrast (PC) MRI [1,2] is the gold standard for MR flow quantification.
  - Partial volume effects;
  - Low SNR.
- Blood flow patterns can also be estimated by model-based computational fluid dynamics (CFD) [3].
  - Arbitrary spatial and temporal resolution;
  - Arbitrary SNR.
- PC generally does not satisfy fluid dynamics equations: momentum and continuity.
- Using MRI measurements to construct a divergence-free flow field was previously described [4,5].
  - Only the z-axis PC velocity component was used to guide CFD solution.
- **Goal**: investigate the use of 3D PC-MRI to guide the CFD calculations.

Numerical Procedure

- Navier-Stokes equation,

$$\rho\left(\frac{\partial \boldsymbol{\nu}}{\partial t}+\boldsymbol{\nu}\cdot\nabla\boldsymbol{\nu}\right)=-\nabla p+\mu\Delta\boldsymbol{\nu}, \qquad (1)$$

  is numerically solved with SIMPLER algorithm [6].
- Discretization of the Navier-Stokes equation yelds three linear systems:

$$\mathbf{A}_{\nu,i}\boldsymbol{\nu}_{i+1}=\mathbf{b}_{\nu,i}, \qquad (2)$$

  for each velocity component $\boldsymbol{\nu}=\mathbf{u}$, $\mathbf{v}$ or $\mathbf{w}$.
- Proposed approach: add rows in the square matrix $\mathbf{A}_{\nu,i}$ incorporating MRI measurements of u, v or w.
- Assumption: MRI-measured velocity within a voxel is a linear combination of the velocities on the CFD grid.
- Systems are solved, for each step of SIMPLER algorithm, in least-square sense.

Experiments

- 3D PC-MRI data were aquired for a carotid flow phantom (Fig.1).
  - 32-channel head coil; resolution: $0.5\times0.5\times1.0$ mm^3; FOV: $4.0\times3.5\times5.0$ cm^3; NEX: 10; Venc: 50 cm/s; scan time: 5 hours.
- Three experiments were performed:
  - Pure CFD solution;
  - Combined solution with MRI measured z velocity component guiding CFD;
  - Combined solution with MRI measured x, y and z velocity components guiding CFD;
- CFD assumptions:
  - $\rho=1100$ kg/m^3; $\mu=0.005$ Pa·s; Voxel size $0.5\times0.5\times1.0$ mm^3.

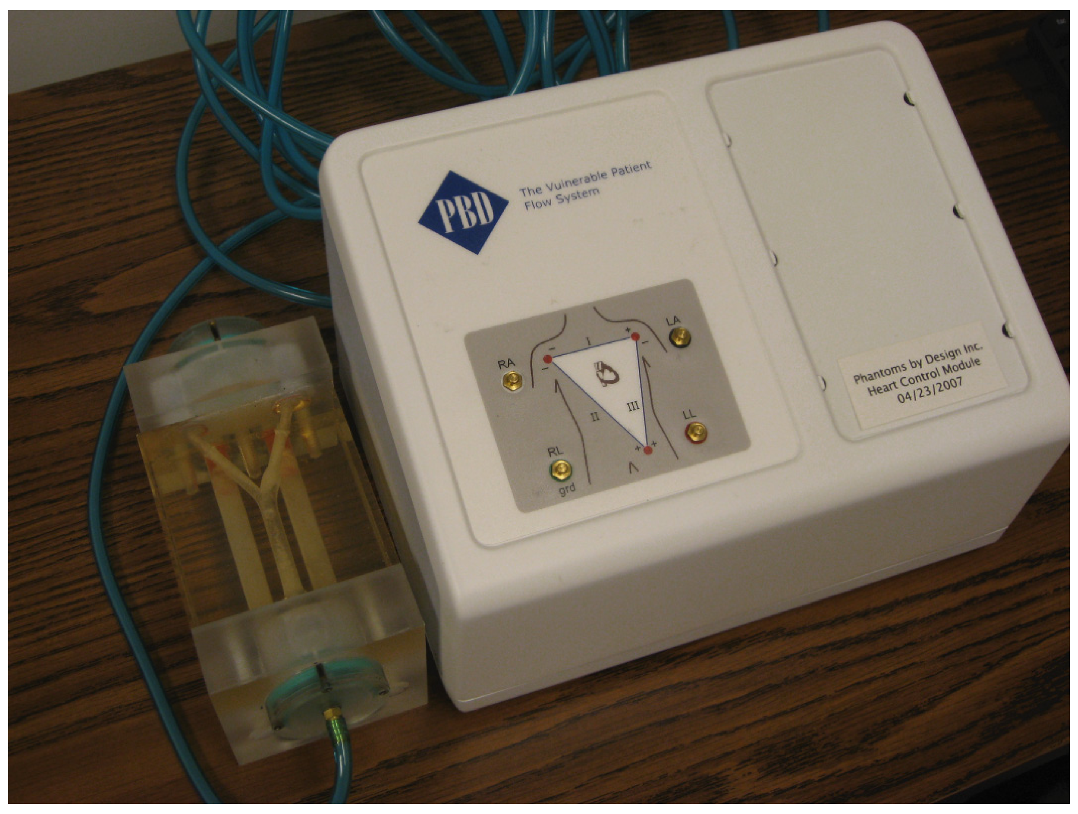

Figure 1: Pulsatile carotid flow phantom (Phantoms by Design, Inc., Bothell, WA).

Results and discussion

- PC-MRI velocity field (Fig.2a) does not satisfy the continuity equation.
- CFD simulations guided by PC-MRI (Fig.2c-d and Fig.3) leads to solutions that are qualitatively more similar to the MRI-measured field, while still satisfying the continuity and momentum equation.
- When all three velocity components are used (proposed approach), the qualitative agreement with PC-MRI is improved for all three components (Fig.2d and Fig.3).
- Signal-to-error ratio (SER) between the CFD solutions and PC-MRI were calculated for u, v, w and $\boldsymbol{\nu}$ (Table 1).
  - Using u_{mri}, v_{mri} and w_{mri} to guide CFD provided better agreement to PC-MRI than other approaches. This approach has 6.56 dB more SER than pure CFD solution and 4.75 dB more SER than combined solution using only w_{mri}.

Conclusion

- Combined solver solutions are closer to PC-MRI than pure CFD solution.
- Corrects the PC-MRI data in order to satisfy both momentum and continuity equation.
- Works as a noise reduction technique (not shown here).
- Easy to implement in Cartesian coordinates.
- Convergence of combined solver solution is approximately 60 times faster than pure CFD solution.

	CFD	CFD + 1D	CFD + 3D
u	2.97 dB	4.16 dB (↑)	6.74 dB (↑)
v	-0.25 dB	-0.30 dB (↓)	2.03 dB (↑)
w	5.44 dB	16.53 dB (↑↑)	13.46 dB (↑)
$\boldsymbol{\nu}=(u,v,w)$	6.57 dB	8.38 dB (↑)	13.13 dB (↑↑)

Table 1: Signal-to-error ratio between PC-MRI phantom data and CFD approaches.

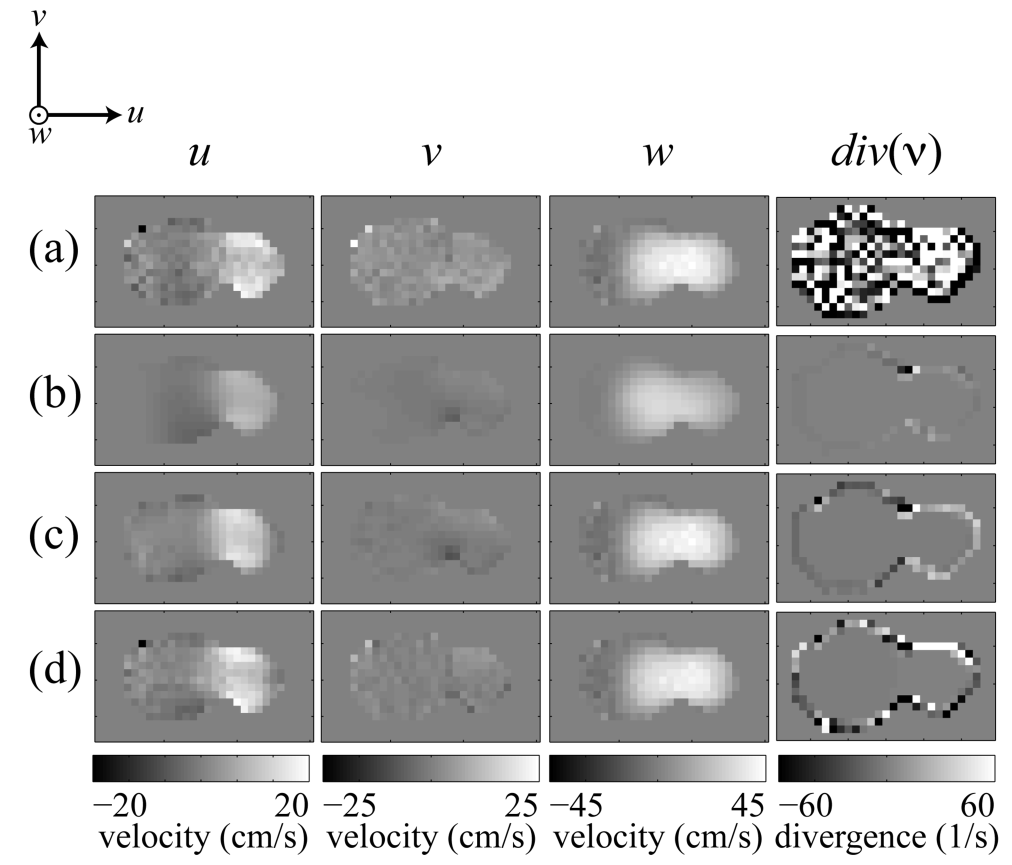

Figure 2: Components and divergence of the velocity field $\boldsymbol{\nu}=(u,v,w)$, at the phantom carotid bifurcation: (a) PC-MRI; (b) CFD; (c) CFD guided by PC-MRI along the z axis; and (d) CFD guided by 3D PC-MRI.

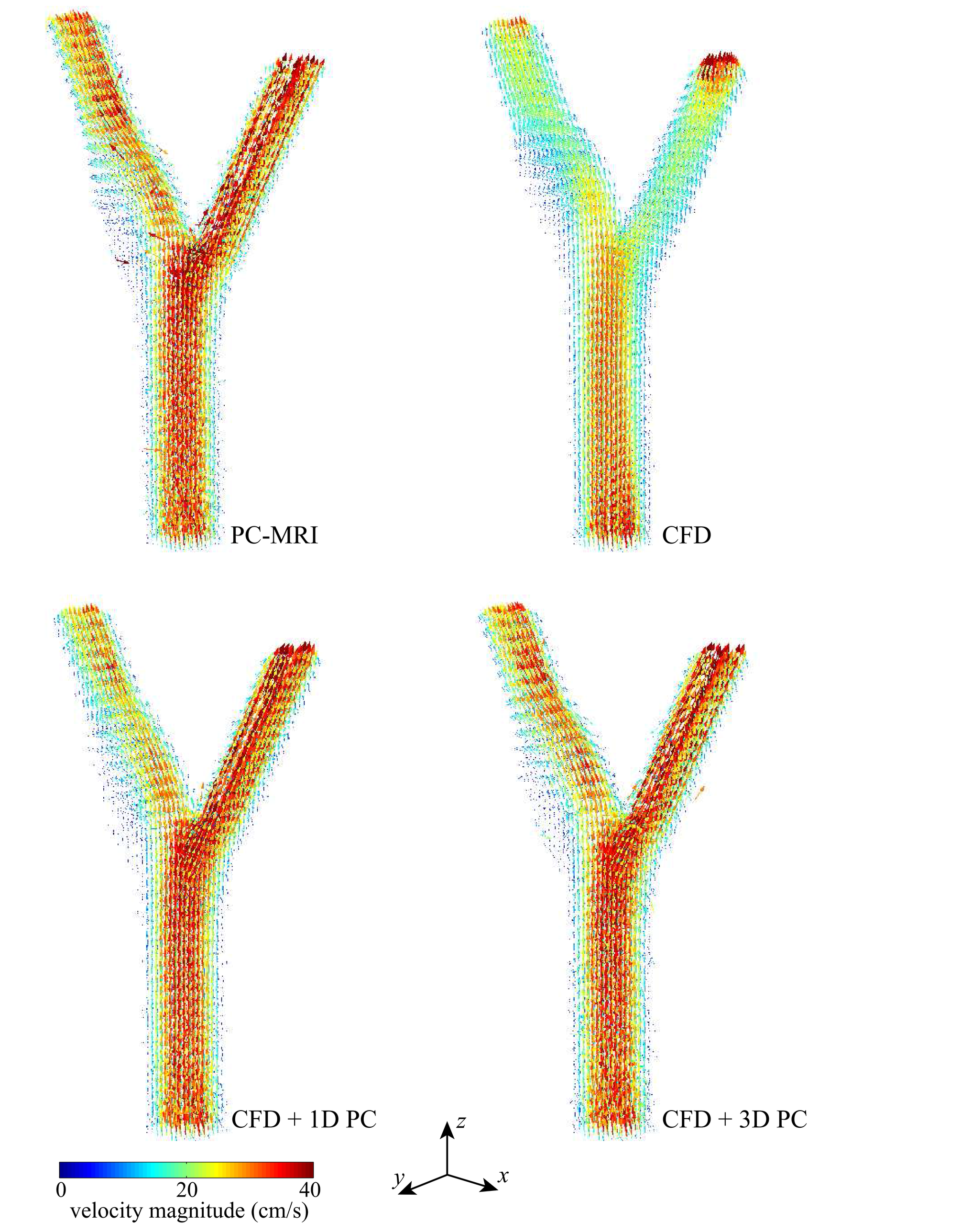

Figure 3: Vector field visualization of carotid flow phantom.

References

[1] O'Donnell M. Med Phys 12:59, 1985.
[2] Markl M et al. JMRI 25:824, 2007.
[3] Rayz VL et al. J Biomech Eng 130:051011, 2008.
[4] Nielsen JF et al. Proc ISMRM 17:3858, 2009.
[5] Rispoli VC et al. Fluid Dynamics, Computational Modeling and Applications 23:513, 2012.
[6] Patankar SV. Numerical Fluid Flow and Heat Transfer, 1980.

Financial support

- Fundação de Apoio à Pesquisa do Distrito Federal: Edital FAP-DF 01/2014